Middle-Pleniglacial soil formation (MIS 3) in the Upper Rhine Graben: The loess-palaeosol sequence of Basel-Schäublinstrasse, Switzerland.

Tina Lander[1], Sally Lowick[2], Christine Pümpin[1] & Philippe Rentzel[1]
[1]Institute for Prehistory and Archaeological Science (IPAS), University of Basel, Switzerland.
philippe.rentzel@unibas.ch, christine.puempin@unibas.ch
[2]Institute of Geological Sciences, University of Bern, Switzerland.

Abstract

In the southern End of the Rhine Graben near Basel (Switzerland), an up to 3 m thick stratigraphy of loess deposits and palaeosols was investigated in a construction pit. Field studies in combination with sedimentology, micromorphology and OSL-dating provided insights on the processes of loess deposition, formation of cambisols (brown earth) and periglacial phenomena around 45 (±5.7) ka. A succession of tundra soils on loess preserving locally foliated organic material can be attributed to the time period between 30.8 (±3.7) ka and 29.4 (±3.4) ka. Furthermore the basal deposit of weathered loess yielded an OSL age which dates back to the Eemian interglacial or the very begining of the last glaciation.

The outcrop of Basel-Schäublinstrasse provided further information to the ongoing studies on loess deposits, regional landscape evolution and environmental conditions during the late Pleistocene in the southern part of the Upper Rhine Plain.

Introduction

The here described stratigraphy is situated in Basel, north-western Switzerland, belonging to the southern End of the Rhine Graben (Fig. 1). South of Basel the hills on the left bank of the Rhine, including the Bruderholz, consist of Tertiary sediments that are overlain by a succession of Pleistocene fluvial terraces (Rentzel *et al.* 2009). The higher terraces, correlated with the cover gravels "Deckenschotter" and the "Hochterrasse" (after the Penck & Brückner scheme, 1901-09), are generally topped by loess deposits up to more than 10 m of thickness (Zollinger 1991). In the past isolated Middle and Upper Palaeolithic artefacts and palaeontological finds were repeatedly observed in the loess deposits of the hills south of Basel (Sedlmeier 2008; Pümpin & Rentzel 2015). Therefore construction sites today are systematically supervised and documented by the archaeological service of the city. The outcrop at Basel-Schäublinstrasse was discovered during such supervision of the excavations for a construction site (Fig. 2). For a short time, the profiles were accessible and could be documented and sampled. The outcrop had a height of 3 m and revealed a loess sequence with several buried soils. The base of the stratigraphy was defined by the depth of the construction pit and is not to be correlated with a specific stratigraphical change in the profile. In the following, we present the first results of palaeopedological and Optically Stimulated Luminescence (OSL) investigations on two selected profiles from Basel-Schäublinstrasse.

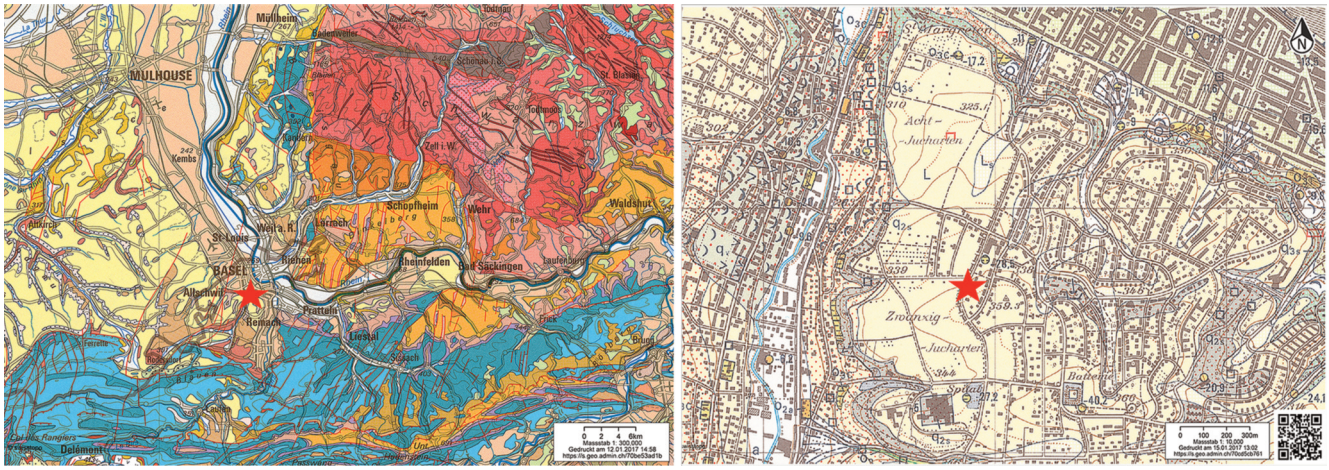

Figure 1: *left: Map of the Rhine Graben with focus on the location of the outcrop Basel-Schäublinstrasse on the Bruderholz hill. Right: Map of the loess deposits (L, yellow signature) of Basel-Schäublinstrasse situated on the Hochterrasse (green signature). (Source: www.map.geo.admin.ch)*

Figure 2: *General view of the outcrop, with the E-Profile (person on the ladder) and on the right site the S-Profile.*

Materials and Methods

During fieldworks in 2014, the outcrop at Basel-Schäublinstrasse was documented by photographing and logging three profiles - i.e. the northern, eastern and southern profile (Fig. 2). The eastern profile, being the reference section, was complemented with information from the southern profile (Fig. 3), as this section reached deeper stratigraphical layers. Sampling of the sections was done directly after cleaning the profiles with respect to the stratigraphy, sedimentology, periglacial features and pedological horizons (Van Vliet-Lanoë 1987; Sponagel 2005; WRB 2007).

Four micromorphological samples were taken from the eastern as well as two from the southern profile. For OSL-dating the eastern profile provided three and the southern one two samples. For sedimentological and geochemical analyses 15 samples were taken from the eastern profile (Fig. 3).

The description of the eight different units the stratigraphy can be divided into is based on observations in the field and was completed by sedimentological as well as geochemical data. The sediments of Units 3, 4, 6 and 7 are present in the micromorphological samples and therefore could be microscopically analysed.

Geochemistry, sedimentology and micromorphology

All 15 samples for geochemical and sedimentological studies were analysed and their results were included in the discussion of the stratigraphy. For micromorphological studies, three samples taken from the eastern profile and the two lowermost ones from the southern profile were impregnated in epoxy resin. A total of 11 thin sections were produced to be examined under a polarising microscope (for further details on the procedure of sample preparation see Rentzel *et al.* 2009). The production of the thin sections was done by the Geoprep laboratory at the University of Basel, Switzerland.

Luminescence dating

Sample preparation and equipment

OSL samples were taken with 25 cm long opaque cylinders in daylight. The outer layers that may have been exposed to daylight were removed and all further work was carried out under subdued orange light in the laboratory. All grains were treated with 32% hydrochloric acid to remove carbonates, 30% hydrogen peroxide to remove any organic component, and sodium oxalate to prevent aggregation of the grains. To isolate the polymineral fine-grained fraction (4-11 µm) samples were settled in Atterberg cylinders using Stokes' law, and a quartz fraction was obtained by immersing a portion of this in 31% hydrofluorosilicic acid for ten days, followed by rinsing with 32% hydrochloric acid to remove fluorides. Grains were settled on stainless discs using acetone.

Measurements were made on automated Risø TL/OSL DA-20 readers, fitted with an EMI 9235QA photomultiplier tube. Stimulation was performed at 90% power, using blue (IR) LEDs for quartz (polymineral), with the signal detected through 7.5 mm of Hoya U-340 transmission filter (410 nm interference filter and one Schott BG-39).

Dose rate determination

400 - 500 g of material was taken from the surrounding sediment for dose rate calculations, and the specific activities of U, Th and K were determined using high-resolution gamma spectrometry (cf. Preusser & Kasper 2001). Concentrations were converted to infinite matrix dose using the conversion factors of Adamiec & Aitken (1998). Cosmic dose was calculated using present day sample burial depth (Prescott & Hutton 1994). An average 40K-content for feldspars of 12.5% was assumed (Huntley & Baril 1997), a-value of 0.07 ± 0.02 for fine grain polymineral samples, and 0.03 ± 0.02 for fine grain quartz (Mejdahl 1987). Present day water content was considered to be representative of the burial period and was used to calculate dose rates.

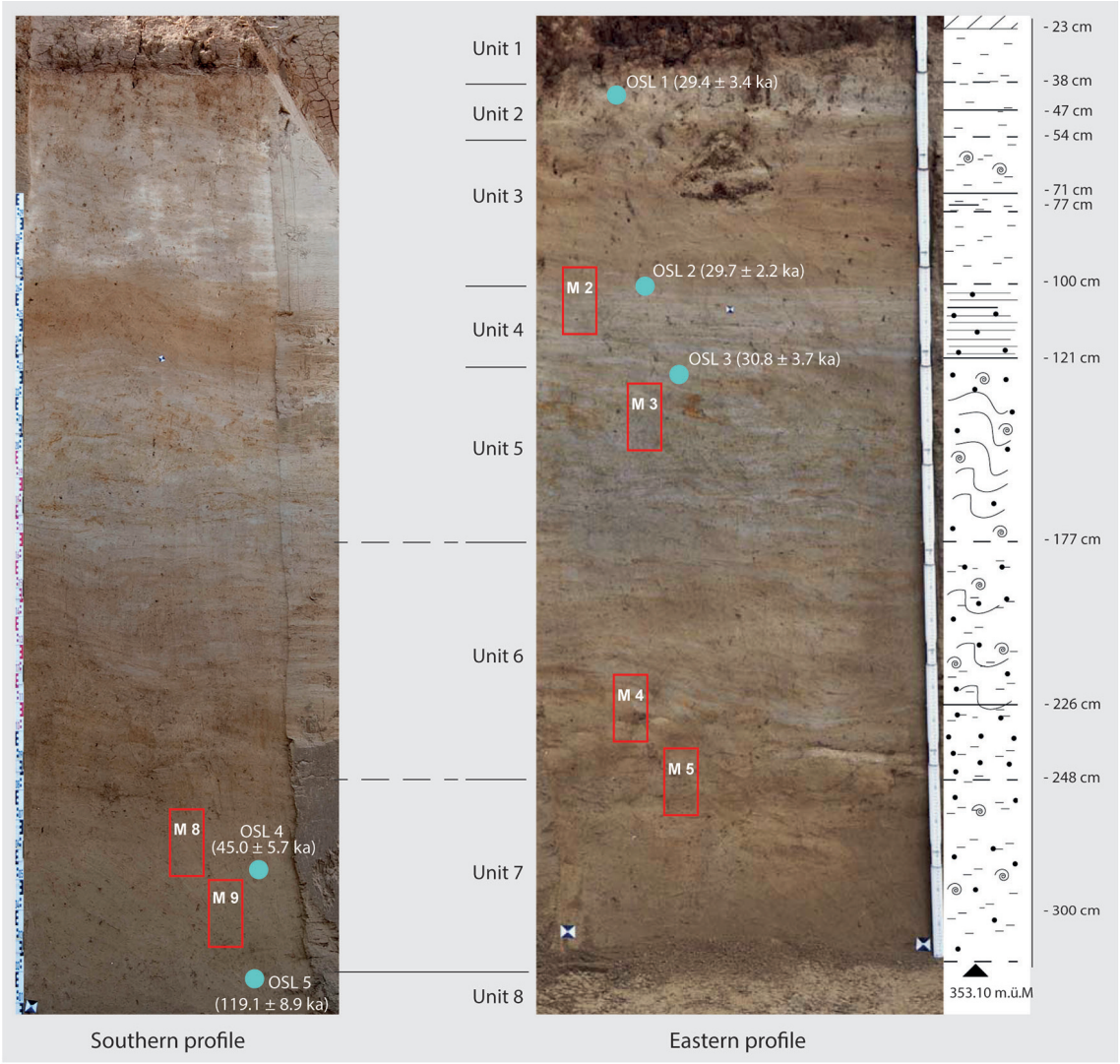

Unit	Colour	CaCo3	Summarised macroscopic & microscopic features	Interpretation
U 1	Dark yellowish brown (10 YR 4/4)	0%	Slightly clayey silt, compact, prismatic structure. Fe precipitations, modern bioturbation. The horizon is artificially truncated.	Truncated Bt-horizon, **Holocene luvisol**.
U 2	Light yellowish brown (10 Y 5/3)	33%	Homogeneous silt. White calcium carbonate precipitations, modern roots.	**Loess**.
U 3	Yellowish brown (10 Y 5/3-6)	20-30%	Compact silt (layered at the bottom), oxidised bands. Contains calcium carbonate precipitations, FeMn precipitations, some fragments of mollusc shells.	**Weathered loess**.
U 4	Light greyish olive brown (2.5 Y 5/4)	20%	Homogeneous, calcareous silt, slightly decalcified. Well-developed platy microstructure with some channels/chambers. Porosity: 15%. Mn impregnations, carbonate hypocoatings, mollusc shells, earthworm biospheroids.	Slightly **weathered loess**, overprinted by frost.
U 5	Light greyish brown (2.5 Y 5/2-6)	32-35%	Geliflucted, calcareous silt with reddish-brown oxidised bands. Platy microstructure. Horizontally bedded organic material, foliated organic components, FeMn impregnations, carbonate hypocoatings, mollusc shells, earthworm biospheroids as well as reworked soil nodules (Bt horizon). Porosity: 5-10%. Isolated fragment of charcoal.	Oxidised loess **tundra gleys.**
U 6	Light greyish brown (2.5 Y 5/4)	31-35%	Compact silt, subhorizontally layered in the upper part. Alternation between light brown and grey, undulated band. Fragments of mollusc shells, FeMn impregnations. In the lower part calcium carbonate precipitations.	Slightly oxidised **loess**.
U 7	Light brown (2.5 Y 5/6)	19-23%	Slightly clayey silt, decalcified. Channel & chamber structure, locally platy microstructure. The lower part of the unit shows freeze-thaw microfabric. FeMn impregnations and reworked FeMn nodules, geliflucted calcite grains with silty cappings, mollusc shells, earthworm biospheroids and calcified root cells as well as carbonate hypocoatings in the upper part of the unit. The middle part contains some rounded soil-aggregates. Lower part with traces of frost-cracks as well as laminated bands of illuviated silt and clay. Porosity: 5-10% (top half) – 15% (bottom half).	**Cambisols**; weathered, bioturbated loess overprinted by frost and gelifluction.
U8	Greyish brown (2.5 Y 5/2)	26%	Homogeneous, unstratified, slightly clayey silt. Weakly decalcified. Slightly humiferous (0.025-0.05 u.c).	**Weathered loess**.

Figure 3: *The southern and eastern profile. In red the samples taken for micromorphological and in blue the samples for OSL analyses. The stratigraphy can be divided into eight units with dates ranging from 119.1 ± 8.9 ka (OSL 5) to 29.4 ± 3.4 ka (OSL 1).*

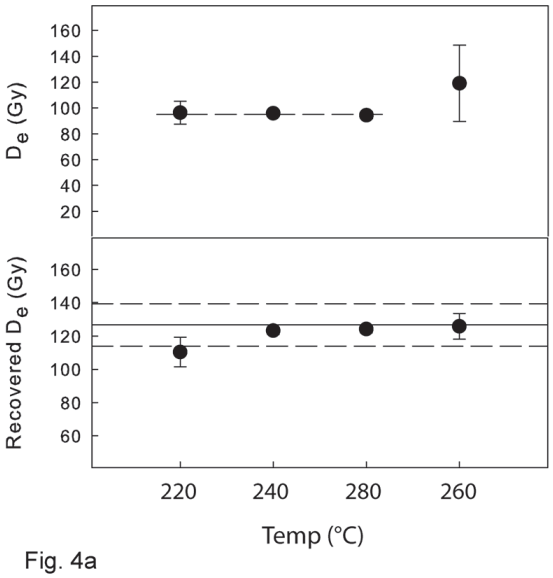

Fig. 4a

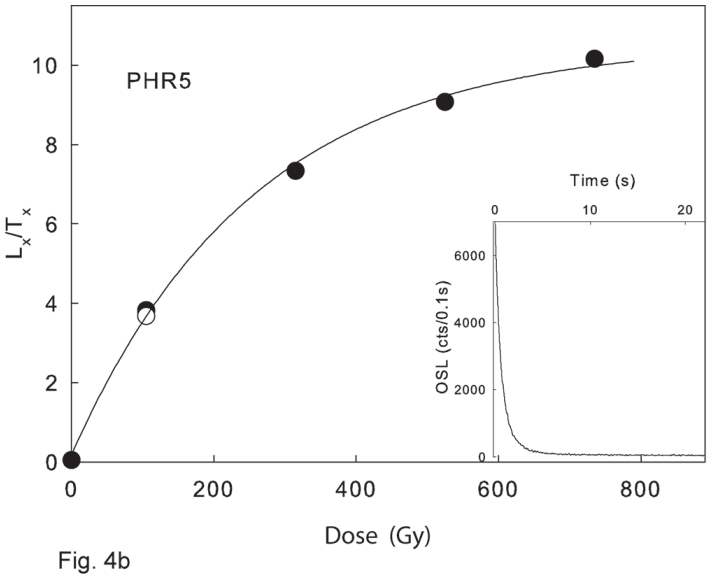

Fig. 4b

OSL Sample	Radionuclide concentration (Bq kg^{-1}) ^{266}Ra	^{232}Th	^{40}K	Water (%)	$D_{(OSL)}$ (Gy ka^{-1})	$D_{e\,(OSL)}$ (Gy)	Age $_{(OSL)}$ (ka)	$D_{(IRSL)}$ (Gy ka^{-1})	$D_{e\,(IRSL)}$ (Gy)	Age $_{(IRSL)}$ (ka)	Corr Age $_{(IRSL)}$ (ka)
OSL1	32.1 ± 0.7	36.1 ± 0.7	318.1 ± 4.2	10	2.6 ± 0.2	77.4 ± 7.1	29.4 ± 3.4	3.1 ± 0.3	69.0 ± 7.0	22.5 ± 3.1	26.4 ± 3.7
OSL2	30.4 ± 0.4	33.1 ± 0.6	298.6 ± 3.8	12	2.4 ± 0.2	71.8 ± 1.9	29.7 ± 2.2	2.8 ± 0.3	61.8 ± 7.2	21.9 ± 3.3	26.1 ± 4.0
OSL3	30.6 ± 0.8	31.3 ± 0.6	276.6 ± 7.2	13	2.3 ± 0.2	70.5 ± 6.5	30.8 ± 3.7	-	-	-	-
OSL4	31.8 ± 0.3	32.2 ± 0.8	279.9 ± 7.7	15	2.3 ± 0.2	103.5 ± 10.6	45.0 ± 5.7	2.6 ± 0.3	105.1 ± 10.7	39.8 ± 5.6	46.4 ± 6.5
OSL5	33.5 ± 0.4	35.3 ± 0.5	302.6 ± 4.6	16	2.4 ± 0.2	284.3 ± 8.3	119.1 ± 8.9	2.8 ± 0.3	255.6 ± 26.3	91.5 ± 12.8	109.6 ± 15.3

Fig. 4c

Figure 4: *a) Preheat (top) and dose recovery (bottom) tests applied to the quartz fraction of OSL4. For the preheat test the dashed line represents the preheat plateau from which a temperature of 240 °C was chosen. For the lower plot, dashed lines represent 10 % errors. b) Dose response curve for the quartz signal of OSL5 together with the decay curve of a natural signal (inset). Empty circle indicates the recycle dose point. OSL dose response curves were well represented by a single saturating exponential (SSE) function, and the luminescence signal showed a rapid decay, confirming that it was dominated by the fast component. This behaviour is representative of all samples. c) Dosimetry information, water content, D_e values and calculated ages. For dosimetry, concentrations were converted to infinite matrix dose using the standard conversion factors of Adamiec and Aitken (1998). Cosmic radiation contribution was calculated using present day sample burial depth following Prescott and Hutton (1994), and attenuation factors were taken from Mejdahl (1987). Water content was as measured. D = Dose rate. OSL = quartz measurements. IRSL = polymineral measurements. Errors on OSL ages represent one standard error. Corr Age (IRSL) = IRSL D_e values correcting for fading using the approach of Huntley & Lamothe (2001), and g-values determined for each sample.*

OSL and IRSL characteristics

All D_e measurements on both quartz and polyminerals were made using modified versions of the SAR protocol (Murray & Wintle 2000, 2003; Wallinga *et al.* 2000; Blair *et al.* 2005). Following preheat and dose recovery tests (Fig. 4a), a preheat of 240°C for 10 s was chosen for all quartz measurements. D_e values were calculated using the first 0.4 s, with the subtraction of a late background calculated using 20-60 s. Aliquots were rejected when the signal was less than three times the background, test dose uncertainty was > 20%, D_e uncertainty was > 30%, recycling ratios were outside > 20% of Unity, and where recuperation values were > 10%. Aliquots that displayed an IR-depletion ratio (Duller 2003) of >20% were rejected.

For $IRSL_{50}$ measurements, a preheat at 250°C for 60 s was used. D_e values were determined using the first 10 s of the IRSL decay curve, with background subtraction calculated using the last 200 s. IRSL dose response curves were represented by a SSE function. Rejection criteria were similar to that for quartz. Fading of the $IRSL_{50}$ signal was determined on three aliquots each of samples OSL-1, 2, 4 and 5 that were sensitised following measurement of D_e. Fading rates were uniform between aliquots and samples, with an average g-value of ~ 1.89 ± 0.47 %, and very similar to previous studies from Switzerland (Gaar & Preusser, 2012; Lowick *et al.* 2010; 2015). D_e values were correcting for fading using the approach of Huntley & Lamothe (2001) and the g-value determined for individual samples.

Observations

D_e values and ages are reported in Fig. 4c, together with the dosimetric data. For both the quartz OSL and the polymineral IRSL, D_e values were all

below ~ 300 Gy, and well below the saturation level of the dose response curves (Wintle and Murray, 2006). While some regions report underestimation of quartz ages above D_e values of ~ 200 Gy (Lai, 2010; Lowick *et al.* 2010; Timar *et al.* 2010), such problems have not been reported for Swiss samples with similar sized D_e values (Dehnert *et al.* 2012; Lowick *et al.* 2015). An example of the OSL dose response curve, and the luminescence decay are shown in Fig. 4b. Quartz OSL and the fading-corrected polymineral IRSL ages are in good agreement and confirm that luminescence signals were fully zeroed prior to burial, as would be expected with wind-blow sediment that has undergone a long transport and exposure to light. The agreement also confirms that the fading correction for the polymineral fraction was successful.

Results

The stratigraphy

Based on the field observations combined with micromorphological, sedimentological and geochemical data, the stratigraphy at Basel-Schäublinstrasse can be divided into eight units (U1-U8 Fig. 3). In the following a short description is presented from base to top:

Unit 8 - Weathered loess (Reworked older loess deposits?)

The sediment of Unit 8, a weathered loessic deposit, resembles macroscopically the overlying loess of Unit 7. However, the difference in colour of the sediments is supporting the hypothesis of a significantly different deposit than the following Unit 7. Unit 8, which is not present in the micromorphological samples, has a much greyer colour than the subsequent sediment of Unit 7 and is slightly less decalcified.

Unit 7 - Weathered loes / Cambisol

Unit 8 is topped by a 50 cm thick partially decalcified silt. Macroscopically homogenous on the whole, it can be subdivided by micromorphological observations. At the base of the unit, the silt appears slightly less weathered than in the upper part of Unit 7. Above the base level, the sediment shows frost cracks as well as laminated bands of illuviated silt and clay: clear signs of frost and potentially gelifluction (Van Vliet Lanoë *et al.* 2004b). Also notable are the already mentioned increasing signs of weathering, as shown by the corrosion on calcite grains, mollusc shells and earthworm granules (biospheroids Fig. 5a-c). Therefore Unit 7 can be classified as a cambisol on loess overprinted by frost and bioturbation.

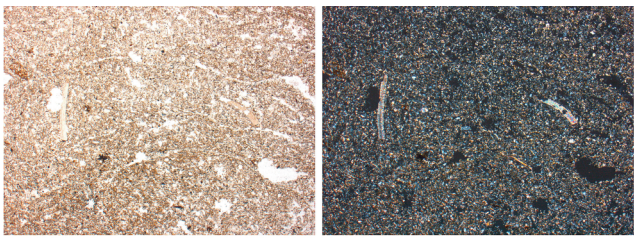
Fig. 5a

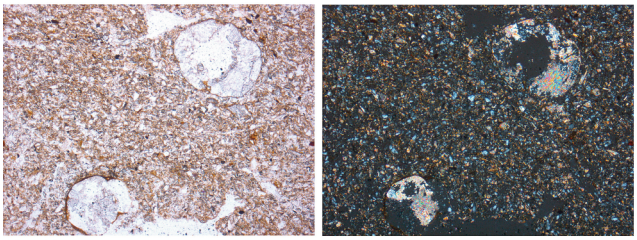
Fig. 5b

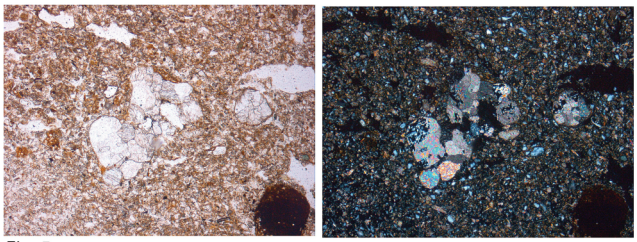
Fig. 5c

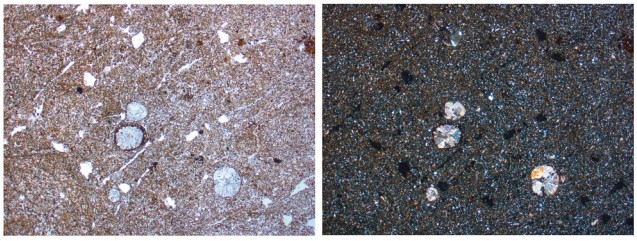
Fig. 5d

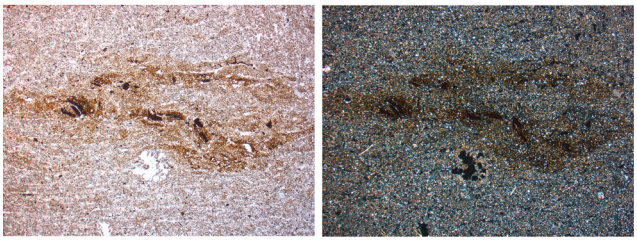
Fig. 5e

Figure 5: *Microphotographs taken in plain polarised light (left) and with crossed polarizers (right). a) Unit 7. Bioturbated loess comprising fragments of weathered mollusc shells. Cambisol with freeze-thaw microfabric. Frame length: 4.5 mm. b) Unit 7. Cambisol comprising corroded biospheroids with silty cappings. Frame length: 2.3 mm. c) Unit 7. Cambisol with weathered biospheroids. Frame length: 2.3 mm. d) Unit 6. Oxidised loess with noticeably less weathered calcitic biospheroids and calcite grains. Frame length: 6.8 mm. e) Unit 5. Oxidised loess with horizontally bedded, foliated organic components. Frame length: 6.8 mm.*

Unit 6 - Oxidised, banded loess

The 70 cm strong Unit 6 is made up of a deposit of unweathered, slightly oxidised loess with high content of calcium carbonate (31-35%). At the base of Unit 6 discrete signs of soil formation and bioturbation appear. Freeze-thaw microfabric, spora-

dical silty cappings on coarser components show that the sediment was overprinted by frost in a periglacial environment (Fig. 5d).

Unit 5 - Oxidised loess / Tundra gleys

The approximately 55 cm thick loess deposit of Unit 5 is composed of geliflucted, calcareous silt showing a reddish-brown oxidised banding as well as horizontally bedded and degraded organic material. Rarely some foliated, dark organic components (Fig. 5e) are present, indicating the existence of former arctic meadows (Van Vliet Lanoë *et al*. 2004a).

Unit 4 - Slightly weathered loess / Tundra soils

The 20 cm thick silty Unit 4 comprises reddish-brown oxidised bandings and foliated organic components as well as very rare fragments of charcoal. In comparison to the oxidised loess (tundra gley) of Unit 5, the sediment of Unit 4 is slightly decalcified. It is composed of a succession of light-brown respectively grey bands, which were macroscopically well visible, as well as periglacial effects in form of gelifluction. Like the tundra gleys of Unit 5, the slightly weathered loess of Unit 4 again indicates an environment of tundra soils overprinted by deep seasonal frost.

Unit 3 - Weathered loess

Unit 3 consists of an about 60 cm thick, homogenous silt. As with the preceding Unit 4, this loess, although calcareous, shows slight decalcification in the lower primarily calcareous 30 cm of the deposit. The upper half however is considerably less decalcified. The sediment sporadically contains reddish-brown bandings of iron impregnations.

Unit 2 - Unweathered loess

The deposit of loess is 15 cm thick and is composed of a homogenous, calcareous windblown silt.

Unit 1 - Holocene luvisol

Partially covered by a modern dump of reworked loamy loess, the 20 cm thick Unit 1 contains the artificially truncated Bt-horizon of the Late Glacial and Holocene luvisol.

Chronology

The sediments of Units 2-5, 7 and 8 were sampled for OSL-dating and yielded important results for the comprehension of late quaternary environmental conditions in the Upper Rhine Graben, particularly as they are correlated with sedimentological and micromorphological observations.

The OSL date of Unit 8 gave an unexpectedly old age of 119 (±8.9) ka (Fig. 4c) placing this layer at the end of the Eemian interglacial or at the beginning of the last glaciation. In any case, the loess deposit of Unit 8 seems to be part of a heavily condensed or even incomplete stratigraphy at the bottom of the outcrop. Unit 8 might be a pedosediment in the form of a colluvium since the strongly developed Eemian luvisol, which is usually present as a regional marker (Zolliger, G., 1991; Jagher *et al.* 2003) is missing in this profile.

The weathered loess of Unit 7 dates to about 45 (±5.7) ka and both the chronological setting as well as the results of the geological analyses hint at a period of periglacial conditions with loess deposition, interrupted by the formation of cambisols during MIS 3. The profile of Basel-Schäublinstrasse contains a succession of well developed soils, although not as clearly pronounced as in the stratigraphies of Datthausen (Sauer *et al.* 2016) or Schwalbenberg in Germany (Profe *et al.* 2016). Further comparable Bw-horizons of cambisols, which date to the same period, can be found at Achenheim near Strasbourg in France (Antoine *et al.* 2001, 223) and in Basel-Riehen (Jagher *et al.* 2003).

The tundra soils of Units 5 and 4 as well as the loess deposits of Units 3 and 2 fall in the period between 30.8 (±3.7) ka and 29.4 (±3.4) ka (Fig. 4c), placing this more than 100 cm and up to 150 cm thick upper part of the stratigraphy at the end of the Middle-Pleniglacial. The paleosols of Units 5 and 4 can be compared to the sequence of Nussloch (Germany) dating around 34 (± 5.7) ka to 29.5 (± 3.7) ka (Antoine *et al.* 2001). At Nussloch, as at Basel-Schäublinstrasse, a Bw-horizon of a cambisol, is followed by several tundra gleys and subsequently by a deposit of calcareous loess. Therefore the strongly developed tundra gleys of Basel-Schäublinstrasse Unit 5 and 4 are likely comparable to the G1 and G2 soils at Nussloch (Antoine *et al.* 2001, 223).

Unit 2 of Basel-Schäublinstrasse marks the beginning of loess accumulation at the very end of MIS 3 and the change to more rigorous conditions. However, the Upper-Pleniglacial loess deposits of MIS 2 which are present at other outcrops such as Sierentz (Rentzel *et al.* 2009) and Allschwil (Zollinger 1991) are barely observed at Basel-Schäublinstrasse. They appear here as a rather thin layer, deeply overprinted by the luvisol which developed during the Late Glacial and Holocene (Brönnimann *et al.* 2015).

Conclusion

The outcrop at Basel-Schäublinstrasse provides an insight into the Middle-Pleniglacial sedimenta-

tion and soil formation processes, providing important information on environmental changes during the late Pleistocene. The results obtained through these loess profiles on the terraces of the Bruderholz hill allow a comparison with other stratigraphies in the region. In addition, the Basel-Schäublinstrasse outcrop may also help to complement missing data from other loess profiles which are only partially dated, for example the stratigraphy of Allschwil (Zollinger 1991).

In comparison to the loess stratigraphies of Datthausen (Sauer *et al.* 2016), Schwalbenberg II (Profe *et al.* 2016), Nussloch (Antoine *et al.* 2001) or Allschwil (Zollinger 1991) the outcrop of Basel-Schäublinstrasse comprises only a relatively short sequence of the complex Quaternary deposits along the Rhine. Nevertheless, the available results permit a better understanding of pedo-sedimentary events during MIS 3 at the southern end of the Rhine Graben during the time-period between 45 and 29 ka, just before the onset of the Last Glacial Maximum.

Acknowledgment

We thank G. Lassau and N. Spichtig, Archaeological Service of Kanton Basel-Stadt (Switzerland) for financial support and for providing technical assistance during field work as well as Susan Steiner for attracting our interest to this temporary outcrop.

References

Adamiec G., Aitken M. (1998) - Dose-rate conversion factors: update. *Ancient* TL 16:37-50.

Antoine P., Rousseau D.-D., Zöller L., Lang A., Munaut A.-V., Hatté Ch., Fontugne M. (2001) - High-resolution record of the last Interglacial-glacial cycle in the Nussloch loess-palaeosol sequences, Upper Rhine Area, Germany. *Quaternary International* 76/77:211-229.

Blair M.W., Yukihara E.G., McKeever S.W.S. (2005) - Experiences with single-aliquot OSL procedures using coarse-grain feldspars. *Radiation Measurements* 39:361-374.

Brönnimann D., Rentzel Ph., Wick L. (2015) - Karstspalte Schachlete. In: Sedlmeier J. (ed.), Die letzten Wildbeuter der Eiszeit: Neue Forschungen zum Spätpaläolithikum im Kanton Basel-Landschaft. *Schriften der Archäologie Baselland* 51:210-241.

Dehnert A., Lowick S.E., Preusser F., Anselmetti F.S., Drescher-Schneider R., Graf H.R., Heller F., Horstmeyer H., Kemna H.A., Nowaczyk N.R., Zügeri A., Furrer H. (2012) - Evolution of an overdeepened trough in the northern Alpine Foreland at Niederweningen, Switzerland. *Quaternary Science Reviews* 34(0), 2012, 127-145.

Duller G.A.T. (2003) - Distinguishing quartz and feldspar in single grain luminescence measurements. *Radiation Measurements* 37(2):161-165.

Gaar D., Preusser F. (2012) - Luminescence dating of mammoth remains from northern Switzerland. *Quaternary Geochronology* 10:257-263.

Huntley D.J., Baril M.R. (1997) - The K content of the K-feldspars being measured in optical dating or in thermoluminescence dating. *Ancient* TL 15:11-13.

Huntley D.J., Lamothe M. (2001) - Ubiquity of anomalous fading in K-feldspars and the measurement and correction for it in optical dating. *Canadian Journal of Earth Sciences* 38:1093-1106.

Jagher R., Rentzel Ph., Schwarz P.-A. (2003) - Ein altsteinzeitliches Geröllartefakt aus Riehen: Ergebnisse der archäologischen und naturwissenschaftlichen Untersuchungen. *Jahresbericht der Archäologischen Bodenforschung des Kantons Basel-Stadt* 2001:103-128.

Lai Z. (2010) - Chronology and the upper dating limit for loess samples from Luochuan section in the Chinese Loess Plateau using quartz OSL SAR protocol. *Journal of Asian Earth Sciences* 37:176-185.

Lowick S.E., Preusser F., Pini R., Ravazzi C. (2010) - Underestimation of fine grain quartz OSL dating towards the Eemian: Comparison with palynostratigraphy from Azzano Decimo, northeastern Italy. *Quaternary Geochronology* 5:583-590.

Lowick S.E., Buechi M.W., Gaar D., Graf H.R., Preusser F. (2015) - Luminescence dating of Middle Pleistocene proglacial deposits from northern Switzerland: methodological aspects and stratigraphical conclusions. *Boreas* 44:459-482.

Mejdahl V. (1987) - Internal radioactivity in quartz and feldspar grains. *Ancient* TL 5:10-17.

Murray A.S., Wintle A.G. (2000) - Luminescence dating of quartz using an improved single-aliquot regenerative-dose protocol. *Radiation Measurements* 32:57-73.

Murray A.S., Wintle A.G. (2003) - The single aliquot regenerative dose protocol: potential for improvements in reliability. *Radiation Measurements* 37:377-381.

Penck A., Brückner E. (1909) - *Die Alpen im Eiszeitalter.* Leipnitz, C. H. Tauchnitz.

Prescott J.R., Hutton J.T. (1994) - Cosmic ray contributions to dose rates for luminescence and ESR dating: Large depths and long-term time variations. *Radiation Measurements* 23:497-500.

Preusser F., Kasper H.U. (2001) - Comparison of dose rate determination using high-resolution gamma spectrometry and inductively coupled plasma-mass spectrometry. *Ancient* TL 19:17-21.

Profe J., Zolitschka B., Schirmer W., Frechen M., Ohlendorf Ch. (2016) - Geochemistry unravels MIS 3/2 paleoenvironmental dynamics at the loess-paleosol sequence Schwalbenberg II, Germany. *Palaeogeography, Palaeoclimatology, Paleoecology* 459:537-551.

Pümpin Ch., Rentzel Ph. (2015) - Schäublinstrasse 115. *Jahresbericht der Archäologischen Bodenforschung des Kantons Basel-Stadt* 2014:66.

Rentzel Ph., Preusser F., Pümpin Ch., Wolf J.-J. (2009) - Loess and palaeosols on the High Terrace at Sierentz (France), and implications for the chronology of terrace formation in the Upper Rhine Graben. *Swiss Journal of Geosciences* 102:387-401.

Sauer D., Kadereit A., Kühn P., Kösel M., Miller Ch. E., Shinonaga T., Kreutzer S., Herrmann L., Fleck W., Starkovich B.M., Stahr K. (2016) - The loess-palaeosol sequence of Datthausen, SW Germany: Characteristics, chronology, and implications for the use of the Lohne Soil as a marker soil. *Catena* 146:10-29.

Sedlmeier J. (2008) - Geheimnisvolle Silexartefakte. In: Archäologische Bodenforschung Basel-Stadt, Historisches Museum Basel (ed.), Unter uns: Archäologie in Basel. Basel, Christoph Merian Verlag, p. 60-64.

Sponagel H. (2005) - *Bodenkundliche Kartieranleitung.* Bundesanstalt für Geowissenschaften und Rohstoffe (Hannover). Ad-hoc-Arbeitsgruppe Boden der geologischen Landesämter und der Bundesanstalt für Geowissenschaften und Rohstoffe der Bundesrepublik Deutschland, 5. verbesserte und erweiterte Auflage, Hannover, Schweizerbart'sche.

Timar A., Vandenberghe D., Panaiotu E.C., Panaiotu C.G., Necula C., Cosma C., van den Haute P. (2010) - Optical dating of Romanian loess using fine-grained quartz. *Quaternary Geochronology* 5:143-148.

Van Vliet-Lanoë B., Magyari A., Meilliez F. (2004a) - Distinguishing between tectonic and periglacial deformations of quaternary continental deposits in Europe. *Global and Planetary Change* 43:103-127.

Van Vliet-Lanoë B., Fox C.A., Gubin St.V. (2004b) - Micromorphology of Cryosols. In: J.M. Kimble (ed.) - *Cryosols: permafrost-affected soils.* Berlin, Heidelberg Springer, p. 365-390.

Van Vliet-Lanoë B. (1987) - Dynamique périglaciaire actuelle et passée apport de l'étude micromorphologique et de l'expérimentation. *Bulletin de l'Assocation française pour l'étude du Quaternaire* 24(3):113-132.

Wallinga J., Murray A., Wintle A. (2000) - The single-aliquot regenerative-dose (SAR) protocol applied to coarse-grain feldspar. *Radiation Measurements* 32(5-6):529-533.

Wintle A.G., Murray A.S. (2006) - A review of quartz optically stimulated luminescence characteristics and their relevance in single-aliquot regeneration dating protocols. *Radiation Measurements* 41:369-391.

WRB (2006) - I.W.G., World reference base for soil resources 2006. A framework for international classification, correlation and communication. Rome: World Soil Resources Reports No. 103, 2006.

Zollinger G. (1991) - Zur Landschaftsgenese und Quartärstratigraphie am südlichen Oberrheingraben: am Beispiel der Lössdeckschichten der Ziegelei in Allschwil (Kanton Basel-Landschaft). *Eclogae Geologicae Helvetiae* 84:739-752.